Hedgehog-responsive mesenchymal clusters direct patterning and emergence of intestinal villi

Katherine D. Walton[a,1], Åsa Kolterud[a,b,1], Michael J. Czerwinski[a], Michael J. Bell[a,c], Ajay Prakash[a], Juhi Kushwaha[a], Ann S. Grosse[a], Santiago Schnell[c], and Deborah L. Gumucio[a,2]

[a]Department of Cell and Developmental Biology, University of Michigan Medical School, Ann Arbor, MI 48109; [b]Department of Biosciences and Nutrition, Karolinska Instituet, Novum, SE-141 83 Huddinge, Sweden; and [c]Department of Molecular and Integrative Physiology, Department of Computational Medicine and Bioinformatics, and Brehm Center for Diabetes Research, University of Michigan Medical School, Ann Arbor, MI 48105

Edited by Brigid L. M. Hogan, Duke University Medical Center, Durham, NC, and approved August 2, 2012 (received for review April 4, 2012)

In the adult intestine, an organized array of finger-like projections, called villi, provide an enormous epithelial surface area for absorptive function. Villi first emerge at embryonic day (E) 14.5 from a previously flat luminal surface. Here, we analyze the cell biology of villus formation and examine the role of paracrine epithelial Hedgehog (Hh) signals in this process. We find that, before villus emergence, tight clusters of Hh-responsive mesenchymal cells form just beneath the epithelium. Cluster formation is dynamic; clusters first form dorsally and anteriorly and spread circumferentially and posteriorly. Statistical analysis of cluster distribution reveals a patterned array; with time, new clusters form in spaces between existing clusters, promoting approximately four rounds of villus emergence by E18.5. Cells within mesenchymal clusters express Patched1 and Gli1, as well as Pdgfrα, a receptor previously shown to participate in villus development. BrdU-labeling experiments show that clusters form by migration and aggregation of Hh-responsive cells. Inhibition of Hh signaling prevents cluster formation and villus development, but does not prevent emergence of villi in areas where clusters have already formed. Conversely, increasing Hh signaling increases the size of villus clusters and results in exceptionally wide villi. We conclude that Hh signals dictate the initial aspects of the formation of each villus by controlling mesenchymal cluster aggregation and regulating cluster size.

epithelial–mesenchymal cross-talk | field pattern | villus morphogenesis

Villi are the functional absorptive units of the small intestine. Their extended epithelial surface provides an enormous area for nutrient absorption, and their cores contain vascular, muscular, nervous, and immune components that are essential for intestinal function. Widespread villus atrophy, as in celiac sprue, can produce severe life-threatening nutrient deficiency (1). Similarly, reduced villus number secondary to significant loss of bowel length can lead to intestinal failure (2). After bowel resection, mechanisms of intestinal adaptation lead to increases in epithelial proliferation and cell migration rate, resulting in longer villi and deeper crypts (3). However, interestingly, the number of villi does not seem to change dramatically, suggesting that the process of villus formation may not occur efficiently in the adult (4, 5).

Villi are first generated during fetal life. Their formation requires epithelial–mesenchymal cross-talk; some of the molecular players in this process have already been identified. Mice lacking the mesenchymal factors Nkx2.3 (6), Foxf1, Foxf2 (7), Foxl1 (previously termed Fkh6) (8), or Pdgfrα (9) exhibit abnormal villi, as do mice deficient in the epithelial factors Ezrin (10) or PdgfA (9). In all these models, villi are generated, although they are aberrant in shape and number. In contrast, we previously reported that villus formation is strongly attenuated in embryonic day (E) 18.5 transgenic founders in which the pan-Hedgehog (Hh) inhibitor, Hhip, is expressed at high levels in the developing intestinal epithelium (11). Recently, conditional deletion of both Shh and Ihh from the gut endoderm was shown to result in nearly complete loss of villi; the very few villi found in this model were thought to arise in areas of incomplete Cre-mediated Shh/Ihh deletion (12). Although these findings suggest that Hh signals likely participate in the generation of villi, several questions remain: Is Hh directly or indirectly required? What is the timing of the Hh requirement? Is Hh required for initiation or extension of villi? What is the nature of the Hh target cells that form the villi?

In this study, we address these open questions by analyzing Hh signal transduction during villus formation in vivo, and by manipulating Hh signaling in an intestinal explant culture model that recapitulates the molecular and morphological events of villus formation in vitro. Our data indicate that epithelial Hh signals are essential for the formation of clusters of mesenchymal cells, without which villus formation fails. Hh acts by promoting the clustering of these Hh-responsive cells and controlling the size of clusters. Additionally, we show that mesenchymal clusters are arrayed in a regular pattern, even before the emergence of villi, indicating that, as in hair (13) or feather formation (14), the intestine uses epithelial/mesenchymal interactions, directed by epithelial Hh signals, to ensure the establishment of a uniform field of villi.

Results

Hh-Responsive Mesenchymal Clusters Form Before Villus Emergence and Adhere Tightly to the Epithelium. Because transgenic mice with reduced Hh signaling exhibit severely curtailed villus formation (11, 12), we sought to determine which cells within the mesenchyme are responsive to Hh signaling before and during villus formation. Using LacZ reporter alleles for *Patched1* (15) and *Gli1* (16), we followed Hh-responsive cells during villus development (E14.0 to E15.5). At E14.0, Hh-responsive cells are scattered throughout the mesenchyme, with a greater concentration closer to the epithelial Hh signal (Fig. 1 *A* and *E*) (17). Half a day later, still before villus emergence, distinct mesenchymal clusters appear, all of which are $Ptc1^+$ and $Gli1^+$ (Fig. 1 *B* and *F*). Shortly thereafter, villi begin to emerge directly above these mesenchymal clusters (Fig. 1 *C* and *G*). In no case was a villus seen to emerge without an associated $Ptc1^+$ (or $Gli1^+$) mesenchymal cluster. Clusters are tightly associated with the epithelial basement membrane at the tips of the growing villi (Fig. 1 *D* and *H*). Transmission electron microscopy (TEM) demonstrates the frequent and intimate association between cells of the mesenchymal clusters and overlying epithelium (Fig. 1 *I* and *J*).

$Pdgfr\alpha^+$ Mesenchymal Clusters Are Targets of Hh Signaling. Because it was previously shown that clusters of mesenchymal cells express Pdgfrα, and that loss of PdgfA/Pdgfrα signaling reduces the number of clusters and villi (9), we examined the extent of overlap between $Pdgfr\alpha^+$ and $Ptc1^+$ clusters. Mice engineered to express the H2B-EGFP fusion protein from the endogenous Pdgfrα locus (18) were mated with the $Ptc1^{LacZ/+}$ and $Gli1^{LacZ/+}$

Author contributions: K.D.W., A.K., and D.L.G. designed research; K.D.W., A.K., M.J.C., J.K., and A.S.G. performed research; K.D.W., M.J.B., A.P., and S.S. contributed new reagents/analytic tools; K.D.W., A.K., M.J.C., M.J.B., A.P., S.S., and D.L.G. analyzed data; and K.D.W. and D.L.G. wrote the paper.

The authors declare no conflict of interest.

This article is a PNAS Direct Submission.

[1]K.D.W. and A.K. contributed equally to this work.

[2]To whom correspondence should be addressed. E-mail: dgumucio@med.umich.edu.

This article contains supporting information online at www.pnas.org/lookup/suppl/doi:10.1073/pnas.1205669109/-/DCSupplemental.

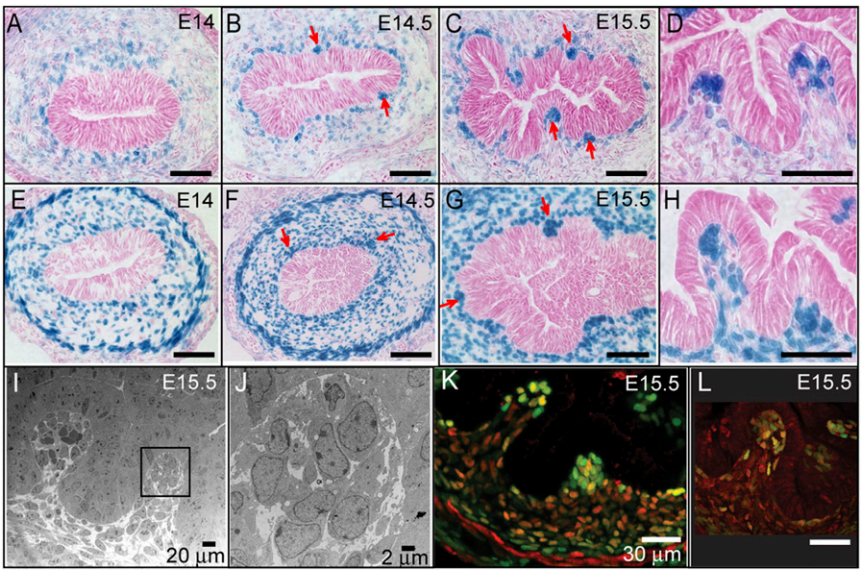

Fig. 1. Mesenchymal clusters are responsive to Hh and PDGF/PDGFRα signaling and are intimately associated with the epithelium. (*A–H*) X-Gal (blue) and eosin (pink) staining of Ptc1$^{LacZ/+}$ (*A–D*) and Gli1$^{LacZ/+}$ (*E–H*) intestines. Red arrows indicate mesenchymal clusters. (*I*) TEM demonstrating association of the cluster with the epithelial basement membrane. (*J*) Magnification of the boxed region in *I*. (*K* and *L*) Cluster cells express PDGFRα (anti-EGFP, green), and Gli1 or Ptc1 (anti-β-gal, red) in PDGFRα$^{EGFP/+}$;Gli1$^{LacZ/+}$ (*K*) or PDGFRα$^{EGFP/+}$;Ptc1$^{LacZ/+}$ (*L*) intestines. (Scale bars, 50 μm, unless indicated otherwise.)

Hh reporter lines and vibratome sections of intestines of mice carrying both marker alleles were analyzed by confocal microscopy (Fig. 1 *K* and *L*). Within the villus clusters, the majority of mesenchymal cells were positive for both Pdgfrα and the Hh reporters; no clusters were seen that were positive for only one of these signaling pathways. However, some mesenchymal cells outside of the clusters were individually responsive to Pdgf or Hh signaling, suggesting that the two pathways both play additional, unique roles during intestinal development.

Mesenchymal Clusters and Villi Form in Wave-Like Fashion, from Anterior to Posterior, Initiating on the Dorsal Side. Previous studies have indicated that villi develop in a proximal-to-distal wave along the length of the intestine (19, 20). We therefore examined whether an anterior-to-posterior wave of cluster formation precedes the formation of villi. At E14.5, E15.5, and E16.5, intestines from Pdgfα$^{EGFP/+}$ mice were isolated and the presence or absence of clusters was assessed along the length of the intestine (Fig. 2*A*). At E14.5, clusters are present within the first 46% of the intestine (10.45/22.43 cm). By E15.5, clusters have formed in the proximal 71% of the intestine (18.71/26.2 cm), and by E16.5, clusters are present through the entire small intestine (47.45 cm). Representative images show the progression of this wave front of cluster formation from jejunum at E14.5 (Fig. S1 *A* and *B*), to proximal ileum at E15.5 (Fig. 2 *B* and *D*), to the ileocecal junction at E16.5 (Fig. 2*C* and Fig. S1*C*). Analysis of the leading front of cluster formation reveals that clusters first form on the dorsal side of the gut tube (marked by the connection to omentum) and spread distally and circumferentially (Fig. 2*E*). Examination of cluster sizes in all areas of the intestine at various stages demonstrates that clusters grow in size as development continues (Table S1). However, clusters associated with nascent villi at any stage in any region of the intestine consistently average 30 μm in diameter [30.15 ± 0.94 (SD) μm in E14.5 duodenum and 30.10 ± 0.80 μm in E16.5 ileum]. Cluster size distribution along the length of the intestine at E15.5 was assessed in opened, flattened intestines (Fig. S2*A*) using Imaris (Bitplane, v7.2). The average area of the 500 largest clusters was greatest in the duodenum and smallest in the ileum, consistent with the existence of a proximal to distal wave of cluster generation (Fig. 2*F*).

A proximal-to-distal wave of villus emergence follows cluster formation. To monitor the wave of villus growth with time, we measured the average length of the longest villi (top 5%) in 8–12 sections of duodenum, jejunum, and ileum at E15.5, E16.5, E17.5, and E18.5. Villi first emerge in the duodenum, then jejunum, and then ileum. Villi in all regions of the intestine continue to lengthen over developmental time (Fig. 2*G*). At all stages, villi are longest in the duodenum and shortest in the ileum and the rate of villus lengthening once villi emerge is similar in all regions up to late gestation. This finding is consistent with a wave of villus growth during fetal life. Although postnatal villus growth was not measured here, differential growth rates after birth could contribute to the fact that villi are shortest in the ileum in the adult (21–23).

Clusters Form in a Patterned Array. Although mesenchymal clusters appear to be regularly distributed, we sought to statistically verify the existence of a patterned arrangement. Quadrat counting (used in point pattern analyses) was used to determine whether the field of clusters is arranged in a regular or random pattern (24, 25). This determination is accomplished by counting the number of clusters in regularly sized quadrats and then calculating the variance-to-mean ratio (VMR) of those counts. If clusters are randomly distributed, the counts and their variances are expected to follow a Poisson distribution, and the VMR will approach 1.0 (24). If the clusters are regularly patterned, the variance among quadrat counts will be small and the VMR will be <1.0.

Quadrat counting of clusters in the duodenum, jejunum, and ileum (three independent fields of each area) yielded VMRs of 0.53, 0.52, and 0.72, respectively, indicating that the clusters are regularly patterned. In a separate set of analyses, images of multiple fields of duodenum were stitched together using Leica LASAF 2.2.0 software to create large fields of clusters, in which over 900 clusters could be counted per field. In this instance, VMR was 0.41, $P \leq 0.001$ compared with 1,000 Monte Carlo simulations. We conclude that, similar to hair, feather, and tooth patterning (13, 14, 26, 27), clusters of Hh-responsive cells are distributed in a patterned array that in turn dictates the later emergence of regularly patterned villi.

Multiple Rounds of Cluster Formation Give Rise to Approximately Four Rounds of Villus Emergence. Sections of intestinal tissue at E15.5 and E16.5, regardless of their orientation, often reveal alternating short and long villi, suggestive of multiple rounds of villus formation (Fig. 3 *A–C*). We examined this result more carefully, from the standpoint of both cluster pattern and villus emergence, to document whether multiple rounds of villus emergence occur and to establish the approximate number of such rounds.

If new clusters form dynamically in the spaces between existing clusters, the nascent clusters are expected to initially be smaller. Thus, in the early patterning field, the nearest neighbor of a small cluster is expected to be a large cluster and vice versa. To quantitatively assess this, we developed a point pattern-analysis function: the neighbor-size correlation function (NSCF). NSCF gives the Pearson correlation of the sizes of neighboring clusters

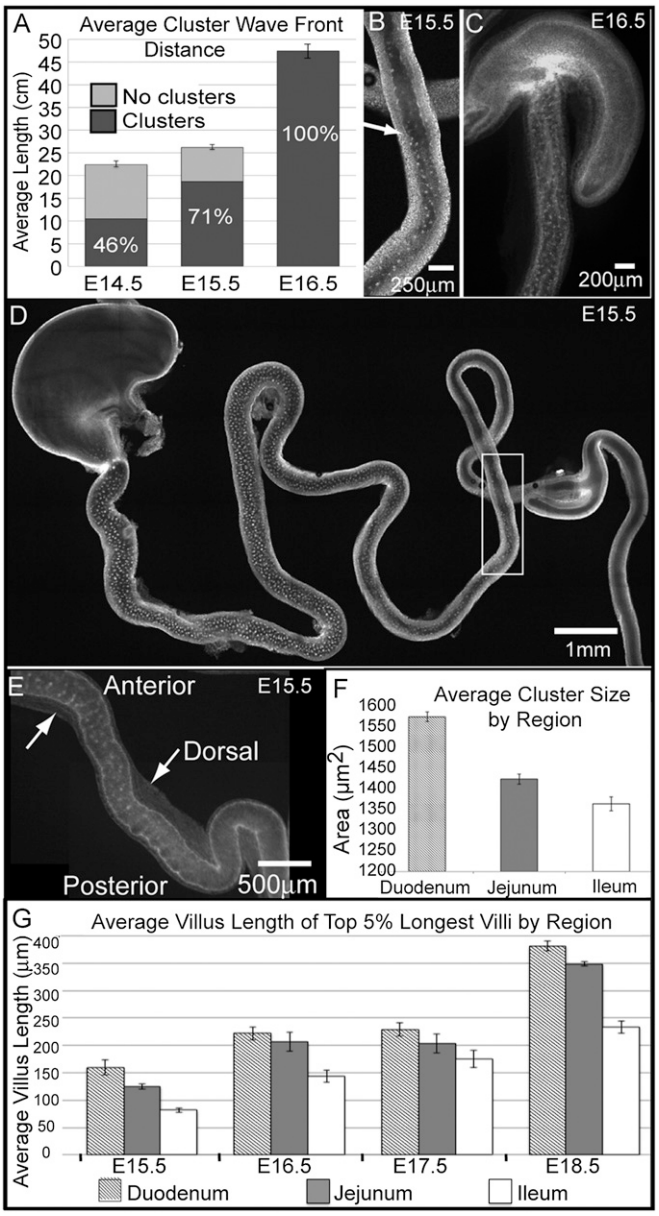

Fig. 2. Cluster formation in PDGFRα$^{EGFP/+}$ intestines occurs in an anterior-to-posterior and dorsal-to-ventral wave. (*A*) Average distance of the cluster wavefront compared with average total small intestine length at E14.5, E15.5, and E16.5. (*B*) Boxed area in *D*, showing the wavefront of cluster formation in the proximal ileum (arrow) at E15.5. (*C*) Cluster formation extends throughout the small intestine by E16.5 (magnified from Fig. S1). (*D*) Three-dimensional reconstruction of five 1-μm *z*-slices from a tiling array of two-photon images of an E15.5 intestine. The figure is a composite to form the full figure. (*E*) At the wave front, clusters predominate on the dorsal side (marked by omentum, arrows). (*F*) Average cluster size (mean ± SD) of the largest 500 clusters per intestinal region at E15.5 ($P < 0.0001$ for all comparisons). (*G*) Average length (mean ± SD) of the longest villi (top 5%) in each region at E15.5 to E18.5. Average longest villus lengths are significantly different among regions at each stage and among regions between stages ($P < 0.001$ for all comparisons); $n = 7{,}020$.

as a function of neighbor distance. The linear dependence between cluster size and neighboring cluster size gives a correlation value between +1 (all clusters are similar in size to their closest neighbors) and −1 (clusters and their nearest neighbors are dissimilar in size). Thus, if multiple rounds of cluster formation occur, we expect neighboring clusters to exhibit a negative NSCF. Indeed, the NSCF is negative up to a distance of nearly 80 μm, indicating that within this distance, large clusters are next to small clusters and vice versa (Fig. S2*C* and Table S2). Interestingly, this negative zone matches well with our direct measurements of average cluster-to-cluster distance of 70.9 ± 0.63 μm (SEM, $n = 670$). Fig. S2*B* shows the correlative data for the search interval that encompasses 40–60 μm. Taken together, these results provide a quantitative assessment of cluster patterning and support the conclusion that multiple rounds of cluster formation occur.

To estimate the number of rounds of villus formation, we first examined the average number of villi per intestinal cross section in 8–12 intestines at E15.5, E16.5, E17.5, and E18.5. At each time point, the number of villi is greatest in the duodenum, less in the jejunum, and fewest in the ileum (Fig. 3*D*). Moreover, for each area of the intestine, the number of villi per cross-section increases with time. These data confirm both the anterior-to-posterior wave of villus emergence and the presence of multiple rounds of villus formation. We next examined the length correlation between all adjacent villi in the duodenum. That value was negative (−0.12 ± 0.045 SEM, $P = 0.009$), as expected if neighboring villi are disparate in size because new villi arise in the space between existing ones. Because, at the earliest stages of villus development (E15.0), we frequently observe four areas of villus emergence per section (Fig. S3 *A* and *A′*), the emergence of a second, third, and fourth round of villi in the spaces between

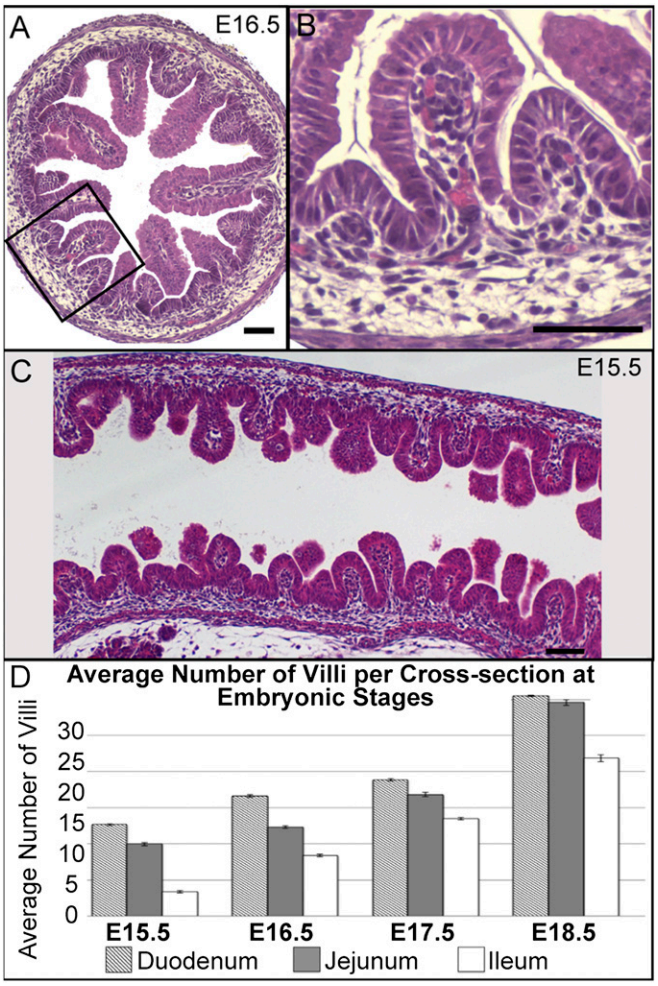

Fig. 3. Multiple rounds of villus emergence occur during fetal development. (*A*) Section of an E16.5 intestine (H&E), showing alternating villus lengths. (*B*) Boxed area in *A*. (*C*) Longitudinal section of an E15.5 intestine (H&E) with alternating villus lengths. (*D*) Average number of villi (mean ± SD) per section in duodenum, jejunum, and ileum at E15.5 to E18.5. (Scale bars, 50 μm.)

existing villi should produce the idealized pattern shown in Fig. S3 *B′–D′*, in which 8, 16, and 32 villi are seen per section. Experimentally, we count a mean ± SEM of 12.6 ± 0.13, 16.6 ± 0.12, and 30.5 ± 0.22 villi at E15.5, E16.5, and E18.5, respectively (Fig. S3 *B–D*). These findings are consistent with the existence of four sequential rounds of villus emergence before birth.

Hh Signaling Controls Cluster Formation and Size. To probe the role of Hh signaling in cluster formation and villus emergence, we developed an organ-culture system based on a modification of the Jaskoll et al. protocol (28). Intestines were dissected from embryos between E13.5 and E14.5 (before the onset of villus formation), placed on transwell membranes, and cultured over media without serum supplement (Fig. S4*A*). Cultured intestines reproducibly developed clusters within 24 h and villi emerged within 48 h (Fig. S4 *B*, *C*, and *G*). Although intestinal viability (measured by cell refractility and peristaltic action) is maintained in this culture system for up to 10 d, the rate of intestinal villus formation slows with time. Thus, the studies here were limited to the first 48 h of culture.

To test whether Hh signals are required for villus formation in this explant system, E13.5 Pdgfrα$^{EGFP/+}$ intestines were treated with cyclopamine, a nontoxic analog, tomatidine, or vehicle and cultured for 48 h. Vehicle- or tomatidine-treated intestines formed clusters and developed villi (Fig. 4 *A*, *B*, *E*, and *H*). However, cyclopamine-treated intestines formed neither clusters nor villi. PDGFRα$^+$ cells are still present in the mesenchyme (Fig. S5), although clusters cannot be detected by either PDGFRα (Fig. 4 *C* and *I*) or by DAPI staining of nuclei (Fig. 4*F*). Interestingly, when the same experiments were performed with E14.5 intestines, in which cluster formation had initiated in the proximal intestine before addition of cyclopamine, clusters associated with nascent villi were seen in the jejunum (Fig. 4 *M* and *P*, and Fig. S6 *E* and *N*). No clusters or villi were seen in the ileum where cluster initiation had not yet begun when treatment was started (Fig. 4*R*, and Fig. S6 *F* and *O*). The clusters seen in the jejunum were more widely spaced than those in control cultures (compare Fig. 4 *M* and *P* with *K*, *L*, and *O*, and Fig. S6 *E* with *D*). These results suggest that Hh signaling is required for the initiation of cluster formation, but not for the emergence of villi if clusters are already formed. The initial round of villus formation requires a Hh signal that is received between E13.5 and E14.5. Continued Hh signaling after E14.5 is required for initiation of subsequent rounds of cluster formation. Inhibition of Hh signaling with the pan-Hh blocking antibody, 5E1, produced similar results (Fig. S6 *S* and *T*).

In parallel experiments, the levels of Hh signaling were increased using the Smoothened agonist, SAG. This treatment resulted in larger, wider clusters that were associated with wider, bulbous villi (Fig. 4 *D*, *G*, and *J*). The average cluster area was significantly larger (36%, $P < 0.0001$) in SAG-treated intestines than in control intestines (Fig. 4*S*). These findings, together with the loss of clusters after inhibition of Hh signaling, indicate that Hh signaling not only initiates mesenchymal cluster formation, but also dictates the size of clusters, thus determining the shape of emerging villi.

Hh Promotes the Aggregation of Mesenchymal Clusters. The above data are consistent with two alternative mechanisms for Hh action in cluster formation: Hh signals may promote the clustering of Ptc1$^+$ cells, or Hh may control the localized proliferation of these cells. To investigate whether clusters form by localized proliferation or by aggregation, we collected 2-h BrdU-labeled intestines at E14.5, E15, E15.5, and E16 and compared the percentage of BrdU$^+$ nuclei within clusters to the percentage of BrdU$^+$ nuclei in scattered mesenchyme cells outside of clusters (Fig. 5 *A–G*). We expected that if clusters were generated by localized proliferation, the percentage of BrdU$^+$ nuclei should be greater in forming clusters than in surrounding mesenchyme. In contrast, if clusters form by aggregation, the BrdU index should be similar in both compartments. At E14.5 when clusters are first beginning to form, this is indeed the case: the percentage of BrdU-labeled cells within clusters is similar to that in unclustered mesenchyme (33% and 36.6%). By E15.0, the BrdU-labeling index seen in clusters is reduced to half of the index seen in unclustered mesenchyme (17.5% vs. 38.5%, $P = 0.0003$). At

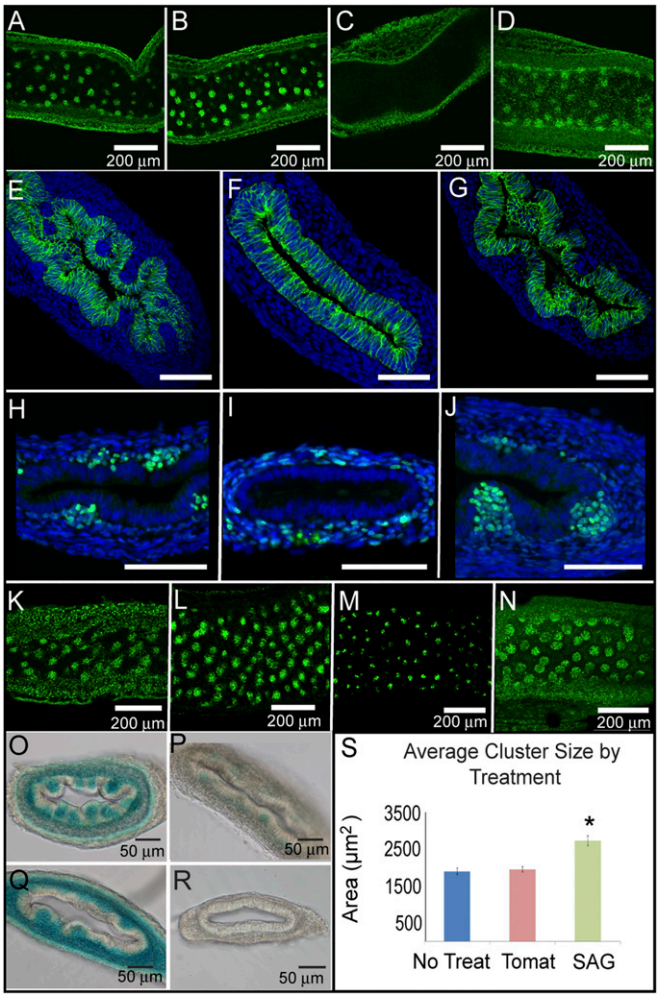

Fig. 4. Hh signaling controls cluster formation and villus size. (*A–J*) E13.5 PDGFRα$^{EGFP/+}$ intestines, cultured for 2 d with vehicle (*A*), 10 μM tomatidine (*B*, *E*, and *H*), 5 μM cyclopamine (*C*, *F*, and *I*), or 1 μM SAG (*D*, *G*, and *J*). (*A–D*) Five-micrometer longitudinal confocal sections of whole intestines. (*E–G*) Sections of intestines with anti–E-cadherin (green) outlining epithelium and DAPI (blue). (*H–J*) Sections with anti-GFP showing PDGFRα$^+$ cluster cells (green) and DAPI (blue). (*K–N*) E14.5 intestines, cultured for 2 d with the same treatments as in *A–D*, respectively. (*O–R*) Vibratome sections of jejunum (*O* and *P*) or ileum (*Q* and *R*) of E14 Ptc$^{LacZ/+}$ intestines cultured with tomatidine (*O* and *Q*) or cyclopamine (*P* and *R*) for 2 d. (*S*) SAG treated intestines have significantly larger clusters (green) than control intestines (red, blue). (*$P < 0.0001$.) Average cluster sizes were no treatment: 1,601 μm^2 ± 155.6 (SEM), $n = 110$; tomatidine: 1,416 μm^2 ± 143.9 (SEM), $n = 139$; SAG: 2,220 μm^2 ± 136.5 (SEM), $n = 143$.

E15.5, very few clusters could be found with BrdU-labeled cells: only 8 of 116 clusters (6.9%) had labeled cells. Within those labeled clusters, only 10.76% of clustered cells were BrdU$^+$. The drop in the number of labeled clusters at later times is likely because of the fact that once clusters mature, cells become postmitotic [Fig. 5*F* and previously shown (9)]. Indeed, we found that many cells in the clusters possess primary cilia (Fig. 5 *H* and *I*), structures that require quiescence to form (29; and reviewed in refs. 30 and 31). Although we cannot rule out the possibility that limited localized proliferation may augment cluster formation, these data are most consistent with the idea that clusters form by aggregation, rather than by localized proliferation. Furthermore, given the loss of clusters after Hh signal reduction and the augmentation in their size with increased Hh signaling, we propose that the function of Hh in cluster formation and subsequent villus emergence is to promote the aggregation of Ptc1$^+$ mesenchymal cells.

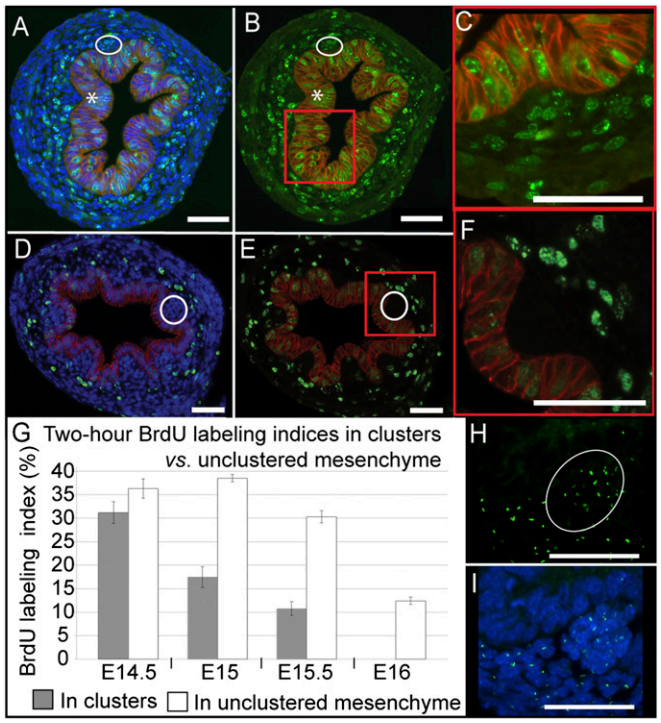

Fig. 5. Mesenchymal clusters of Hh-responsive cells form by aggregation. (*A–F*) Sections of 2-h BrdU-labeled E15.0 (*A–C*) or E15.5 (*D–F*) duodenum stained with anti-BrdU (green), anti–E-cadherin (red), and DAPI (blue). White circles outline clusters. (*C* and *F*) Magnifications of boxed areas in *B* and *E*, respectively. Note the postmitotic cluster (asterisk in *B*). (*G*) BrdU labeling indices (mean ± SEM) at different stages in clusters (gray) vs. unclustered mesenchyme (white). (*H* and *I*) Anti-Arl13b marks primary cilia in mesenchymal clusters (green) and DAPI marks nuclei (blue). (Scale bars, 50 μm.)

Discussion

Although the literature from the early 1900s describing villus development includes references to "mesenchymal growths that push toward the epithelium" (19, 20), the presence of discrete knots or clusters of subepithelial mesenchymal cells in association with forming villi was first documented by Mathan et al. in 1976 (32). Later, Karlsson et al. demonstrated that the cells within these clusters possess Pgdfα receptors, and that the loss of Pdgfrα or its ligand, PdgfA, affects the number and shape of emerging villi but does not prevent formation of the first round of villi (9). Here, we characterize the initiation of villus formation in greater depth and are unique in showing that the clusters associated with emerging villi also transduce Hh signals. Moreover, we demonstrate that elimination of the Hh signal before mesenchymal aggregation completely abrogates villus emergence. Furthermore, the level of Hh signaling dictates mesenchymal cluster size and thus, villus shape. Given the morphological similarity of mouse and human intestine and the significant overlap in intestinal gene expression in these two species, it is likely that mechanistic characterization of villus formation in the mouse model will be directly applicable to the human intestine.

An important contribution of the work we present here is the establishment of quantitative measurements of patterning in the developing mouse intestine. We used these measurements to show that mesenchymal clusters in the developing intestine are indeed regularly distributed and that sequential rounds of cluster formation dictate four rounds of villus emergence between E14.5 and E18.5. We also established baseline values for villus height at daily time points between E14.5 and E18.5 and for the average spacing within the field of mesenchymal clusters. Quantitation of these complex elements of tissue pattern is essential to establish a ruler against which to accurately compare perturbances in the system.

The intestinal mesenchymal clusters have several similarities to the mesenchymal condensates involved in the patterning of hair, teeth, tongue papillae, feathers, and hair follicles (13, 26, 33–39). Like the dermal condensates associated with feather formation in the chick, villus clusters first arise in anterior and dorsal midline regions and then spread posteriorly and laterally (33). Also like dermal condensates, the regular timing and spacing of mesenchymal clusters implies the existence of specific patterning signals. We have identified Hh as one of these patterning signals. An important next challenge will be to decipher the mesenchymal signals acting downstream of Hh. The transcription factors *Foxf1* and *Foxl1* have been identified as direct Hh target genes (40), and both genes are expressed in the fetal intestinal mesenchyme, in a similar pattern as *Ptc1* (41, 42). Targeted inactivation of *Foxf1* or *Foxl1* results in an abnormal intestinal architecture with irregularly shaped villi (7, 8). It is possible that the villus-inducing role of Hh is mediated at least in part by *Foxf1* and *Foxl1*.

In the context of villus patterning, it is interesting to consider that the first round of villus emergence occurs under somewhat different circumstances than all subsequent rounds (Fig. S7). Initially, mesenchymal clusters form beneath a highly proliferative pseudostratified epithelium that is uniformly expressing Shh, Ihh, and PdgfA (9, 17, 43). These initial clusters are regularly spaced, as shown by our pattern analysis, although the mechanisms that determine their initial positioning and even distribution have yet to be elucidated. After the initial clusters are generated, the positions of secondary, tertiary, and quaternary clusters must be dictated by the patterning field that has been already established. The regular pattern that we measure suggests that formation of the later clusters, which must be positioned in the intervillus regions between already emerged villi, is actively inhibited until the proliferative intervillus regions grow to a size that can accommodate expansion of the patterning field. Thus, it is possible that some of the molecular factors that dictate the formation and patterning of the first round of clusters differ from those that are responsible for all subsequent rounds, although a requirement for Hh signaling seems to pervade all rounds.

For all rounds of villus formation, the tight association between the mesenchymal cluster and the epithelium is striking. This intimate contact between the cluster and the epithelium, coupled with the finding that when clusters are lost (as after interruption of Hh signaling) villi fail to form, supports the conclusion that cross-talk between epithelium and mesenchyme is critical for the process of villus emergence. Findings from recent organoid cultures further reinforce this hypothesis. Single adult epithelial stem cells placed in culture are capable of forming organoids that contain crypts, but not villi (44), suggesting that although crypts are self-organizing, villi are not. In contrast, when gut organoids are formed from the differentiation of embryonic stem cells into both endodermal and mesenchymal derivatives, these structures do contain villi (45). This close interaction and interdependence of epithelium and mesenchyme may help to ensure that every emerging villus is properly endowed with a mesenchymal core that is required for absorptive function.

Materials and Methods

Mice. All protocols for mouse experiments were approved by the University of Michigan Unit for Laboratory Animal Medicine. Gli1$^{LacZ/+}$, Ptc1$^{LacZ/+}$, and PDGFRα$^{EGFP/+}$ mice have been described previously (15, 16, 18) and are available through the Jackson Laboratory (strains 008211, 003081, and 007669, respectively).

Organ Culture. Organ cultures were performed according to our modification of the method of Jaskoll et al. (28). Briefly, E13.5 or E14.5 intestines were dissected from the embryos in cold DPBS (Invitrogen 14040-133), connective tissue was separated, and intestines were placed on transwells (Costar 3428) in BGJb media (Invitrogen 12591-038) supplemented with 1% pen/strep (vol/vol) (Invitrogen 15140-122) and 0.1 mg/mL ascorbic acid. Intestines were cultured for 24–48 h (as indicated in the figure legends) at 37 °C with 5% CO_2 with media changes every 12 h.

Drugs. Drugs were purchased as follows: Tomatidine (Calbiochem 614350), Cyclopamine (LC Laboratories C-8700), and SAG (Enzo Life Sciences ALX-270–426-M001).

TEM. E15.5 intestines were fixed in 2.5% (wt/vol) glutaraldehyde in 0.1 M Sorensen's buffer, pH 7.4, overnight at 4 °C. After postfixation in 1% (wt/vol) osmium tetroxide, tissues were rinsed and stained en bloc with aqueous 3% (wt/vol) uranyl acetate for 1 h, dehydrated in ethanol, rinsed in propolynoxide, and embedded in epoxy resin. Sections (70 nm) were stained with uranyl acetate and lead citrate and examined using a Philips CM100 electron microscope.

X-Gal Staining. X-Gal staining of sectioned tissues was performed as described previously (17). Whole-mount tissues were fixed in 4% (wt/vol) PFA for 10 min, washed in PBS and X-Gal stained as previously described (17).

Vibratome Sectioning. Fixed intestines were embedded in 7% (wt/vol) low-melt agarose (Sigma A9414) in PBS and vibratome sectioned at 100 μM.

Immunostaining. Antibodies were: chicken anti–β-galactosidase 1:1,000 (AbCam ab9361), goat anti-GFP 1:1,000 (AbCam ab6662), mouse anti-Ecadherin 1:1,000 (BD 610182), rabbit anti-Arl13b 1:1,500 [kind gift from Tamara Caspary (Emory University, Atlanta, GA)], mouse anti-BrdU 1:400 (DSHB G3G4), or rat anti-BrdU 1:200 (Accurate OBT0030G).

Quadrat Counting and NCSF Analysis. Clusters were counted in a set of n quadrats within an image of intestine. The number of clusters, x_i , were counted in the i th quadrat. The mean and sample variance were calculated as in ref. 46.

NCSF was implemented in a program written in R (47) to compute the Pearson correlation: Let S_V be an ordered list of the size of every cluster within a region of interest. Let r_i denote the i^{th} term in an ordered list of increasing radial distances (e.g., $r_0 = 0$ μm, $r_1 = 10$ μm, $r_2 = 20$ μm,. . ., $r_n = 10 \times n$ μm). For each cluster in S_V, let N_i be the average size of neighbors whose centers lie at a distance between r_i and r_{i-1} from that cluster. Let S_i be an ordered list of the average neighbor sizes N_i for each cluster. Then the NCSF gives the correlation of S_v with S_i on the interval r_{i-1} to r_i. See Table S2 for NSCF values, SEM and P values.

BrdU (50 mg/kg) was intraperitoneally injected into pregnant females at the stages indicated within the text and prepared as described previously (43).

ACKNOWLEDGMENTS. We thank Drs. Benjamin Allen, William Zacharias, Aaron Udager, and Milena Salces-Saqui for providing helpful advice; and Jierong Lang, Nishita Parmar, and Michelle Durance for providing technical support. Imaging and analysis were performed in the Microscopy and Image Analysis Laboratories at the University of Michigan and the Morphology and Image Analysis Core of the Michigan Diabetes Research and Training Center, supported by P60 DK-20572. Funding support was provided by Grants R01 DK065850, T32-HL07622, and T32-HL07505.

1. Cárdenas A, Kelly CP (2002) Celiac sprue. *Semin Gastrointest Dis* 13:232–244.
2. Miyasaka EA, Brown PI, Teitelbaum DH (2011) Redilation of bowel after intestinal lengthening procedures—An indicator for poor outcome. *J Pediatr Surg* 46:145–149.
3. Yang H, Antony PA, Wildhaber BE, Teitelbaum DH (2004) Intestinal intraepithelial lymphocyte gamma delta-T cell-derived keratinocyte growth factor modulates epithelial growth in the mouse. *J Immunol* 172:4151–4158.
4. Forrester JM (1972) The number of villi in rat's jejunum and ileum: Effect of normal growth, partial enterectomy, and tube feeding. *J Anat* 111:283–291.
5. Clarke R (1967) On the constancy of the number of villi in the duodenum of the post-embryonic domestic fowl. *J Embryol Exp Morphol* 17:131–138.
6. Pabst O, Zweigerdt R, Arnold HH (1999) Targeted disruption of the homeobox transcription factor Nkx2-3 in mice results in postnatal lethality and abnormal development of small intestine and spleen. *Development* 126:2215–2225.
7. Ormestad M, et al. (2006) Foxf1 and Foxf2 control murine gut development by limiting mesenchymal Wnt signaling and promoting extracellular matrix production. *Development* 133:833–843.
8. Kaestner KH, Silberg DG, Traber PG, Schütz G (1997) The mesenchymal winged helix transcription factor Fkh6 is required for the control of gastrointestinal proliferation and differentiation. *Genes Dev* 11:1583–1595.
9. Karlsson L, Lindahl P, Heath JK, Betsholtz C (2000) Abnormal gastrointestinal development in PDGF-A and PDGFR-(alpha) deficient mice implicates a novel mesenchymal structure with putative instructive properties in villus morphogenesis. *Development* 127:3457–3466.
10. Saotome I, Curto M, McClatchey AI (2004) Ezrin is essential for epithelial organization and villus morphogenesis in the developing intestine. *Dev Cell* 6:855–864.
11. Madison BB, et al. (2005) Epithelial hedgehog signals pattern the intestinal crypt-villus axis. *Development* 132:279–289.
12. Mao J, Kim BM, Rajurkar M, Shivdasani RA, McMahon AP (2010) Hedgehog signaling controls mesenchymal growth in the developing mammalian digestive tract. *Development* 137:1721–1729.
13. St-Jacques B, et al. (1998) Sonic hedgehog signaling is essential for hair development. *Curr Biol* 8:1058–1068.
14. Ting-Berreth SA, Chuong CM (1996) Sonic Hedgehog in feather morphogenesis: Induction of mesenchymal condensation and association with cell death. *Dev Dyn* 207:157–170.
15. Goodrich LV, Milenković L, Higgins KM, Scott MP (1997) Altered neural cell fates and medulloblastoma in mouse patched mutants. *Science* 277:1109–1113.
16. Bai CB, Auerbach W, Lee JS, Stephen D, Joyner AL (2002) Gli2, but not Gli1, is required for initial Shh signaling and ectopic activation of the Shh pathway. *Development* 129:4753–4761.
17. Kolterud A, et al. (2009) Paracrine Hedgehog signaling in stomach and intestine: New roles for hedgehog in gastrointestinal patterning. *Gastroenterology* 137:618–628.
18. Hamilton TG, Klinghoffer RA, Corrin PD, Soriano P (2003) Evolutionary divergence of platelet-derived growth factor alpha receptor signaling mechanisms. *Mol Cell Biol* 23:4013–4025.
19. Johnson FP (1910) The development of the mucous membrane of the oesophagus, stomach, and small intestine in the human embryo. *Am J Anat* 10:55.
20. Kammeraad A (1942) The development of the gastrointestinal tract of the rat. I. Histogenesis of the epithelium of the stomach, small intestine and pancreas. *J Morphol* 70:29.
21. Abbas B, Hayes TL, Wilson DJ, Carr KE (1989) Internal structure of the intestinal villus: Morphological and morphometric observations at different levels of the mouse villus. *J Anat* 162:263–273.
22. Wołczuk K, Wilczyńska B, Jaroszewska M, Kobak J (2011) Morphometric characteristics of the small and large intestines of *Mus musculus* during postnatal development. *Folia Morphol (Warsz)* 70:252–259.
23. FitzSimmons J, Chinn A, Shepard TH (1988) Normal length of the human fetal gastrointestinal tract. *Pediatr Pathol* 8:633–641.
24. Pielou EC (1977) *Mathematical Ecology* (John Wiley & Sons, New York).
25. Cressie NA ed (1991) *Statistics for Spatial Data* (John Wiley & Sons, New York), Revised Ed.
26. Dassule HR, Lewis P, Bei M, Maas R, McMahon AP (2000) Sonic hedgehog regulates growth and morphogenesis of the tooth. *Development* 127:4775–4785.
27. Gritli-Linde A, et al. (2002) Shh signaling within the dental epithelium is necessary for cell proliferation, growth and polarization. *Development* 129:5323–5337.
28. Jaskoll TF, Don-Wheeler G, Johnson R, Slavkin HC (1988) Embryonic mouse lung morphogenesis and type II cytodifferentiation in serumless, chemically defined medium using prolonged in vitro cultures. *Cell Differ* 24:105–117.
29. Tucker RW, Scher CD, Stiles CD (1979) Centriole deciliation associated with the early response of 3T3 cells to growth factors but not to SV40. *Cell* 18:1065–1072.
30. Kobayashi T, Dynlacht BD (2011) Regulating the transition from centriole to basal body. *J Cell Biol* 193:435–444.
31. Kim S, Tsiokas L (2011) Cilia and cell cycle re-entry: More than a coincidence. *Cell Cycle* 10:2683–2690.
32. Mathan M, Moxey PC, Trier JS (1976) Morphogenesis of fetal rat duodenal villi. *Am J Anat* 146:73–92.
33. Sengel P (1976) *Morphogenesis of Skin* (Cambridge Univ Press, New York).
34. Dhouailly D (1977) Dermo-epidermal interactions during morphogenesis of cutaneous appendages in amniotes. *Frontiers of Matrix Biology*, ed Robert L (S. Karger, New York), Vol 4, pp 85–121.
35. Jiang TX, Jung HS, Widelitz RB, Chuong CM (1999) Self-organization of periodic patterns by dissociated feather mesenchymal cells and the regulation of size, number and spacing of primordia. *Development* 126:4997–5009.
36. Chuong CM, Patel N, Lin J, Jung HS, Widelitz RB (2000) Sonic hedgehog signaling pathway in vertebrate epithelial appendage morphogenesis: perspectives in development and evolution. *Cell Mol Life Sci* 57:1672–1681.
37. Scaal M, et al. (2002) BMPs induce dermal markers and ectopic feather tracts. *Mech Dev* 110:51–60.
38. Mikkola ML, Millar SE (2006) The mammary bud as a skin appendage: Unique and shared aspects of development. *J Mammary Gland Biol Neoplasia* 11:187–203.
39. Michon F, Forest L, Collomb E, Demongeot J, Dhouailly D (2008) BMP2 and BMP7 play antagonistic roles in feather induction. *Development* 135:2797–2805.
40. Madison BB, McKenna LB, Dolson D, Epstein DJ, Kaestner KH (2009) FoxF1 and FoxL1 link hedgehog signaling and the control of epithelial proliferation in the developing stomach and intestine. *J Biol Chem* 284:5936–5944.
41. Mahlapuu M, Enerbäck S, Carlsson P (2001) Haploinsufficiency of the forkhead gene Foxf1, a target for sonic hedgehog signaling, causes lung and foregut malformations. *Development* 128:2397–2406.
42. Sackett SD, Fulmer JT, Friedman JR, Kaestner KH (2007) Foxl1-Cre BAC transgenic mice: A new tool for gene ablation in the gastrointestinal mesenchyme. *Genesis* 45:518–522.
43. Grosse AS, et al. (2011) Cell dynamics in fetal intestinal epithelium: Implications for intestinal growth and morphogenesis. *Development* 138:4423–4432.
44. Sato T, et al. (2009) Single Lgr5 stem cells build crypt-villus structures in vitro without a mesenchymal niche. *Nature* 459:262–265.
45. Spence JR, et al. (2011) Directed differentiation of human pluripotent stem cells into intestinal tissue in vitro. *Nature* 470:105–109.
46. Cox DR, Lewis PAW (1966) *The Statistical Analysis of Series of Events* (Methuen, London), p viii, 285 pp.
47. Team RDC (2010) *R: A Language and Environment for Statistical Computing* (R Foundation for Statistical Computing, Vienna, Austria).